Int. J. Electrochem. Sci., 8 **(2013)** 6775 - 6783

International Journal of
ELECTROCHEMICAL
SCIENCE
www.electrochemsci.org

High Power $LiMn_2O_4$ Hollow Microsphere Cathode Materials for Lithium Ion Batteries

Chen Wei[1], *Jianqiu Deng*[1,*], *Liujiang Xi*[2], *Huaiying Zhou*[1], *Zhongmin Wang*[1], *C.Y. Chung*[2], *Qingrong Yao*[1], *Guanghui Rao*[1]

[1] School of Material Science and Engineering, Guilin University of Electronic Technology, Guilin 541004, China
[2] Department of Physics & Materials Science, City University of Hong Kong, Tat Chee Avenue, Kowloon, Hong Kong SAR, China
[*]E-mail: jqdeng@guet.edu.cn

Received: 10 March 2013 / *Accepted:* 28 March 2013 / *Published:* 1 May 2013

Lithium manganese oxide ($LiMn_2O_4$) hollow microspheres have been synthesized by using $MnCO_3$ precursor as a self-template. The microstructure of the hollow microspheres is characterized by X-ray diffraction and environmental scanning electron microscopy. The electrochemical performance of the samples is evaluated by cyclic voltammetry and charge-discharge cycling tests. $LiMn_2O_4$ hollow microspheres deliver excellent cycling stability and rate capability. The initial discharge capacity is 61.5 $mAhg^{-1}$ tested at a rate of 20C. The capacity retention ratio is above 87% after 1200 charge-discharge cycles. The results indicate the $LiMn_2O_4$ hollow microspheres are the most promising cathode materials, which may be used in high power lithium ion batteries.

Keywords: Lithium-ion battery; $LiMn_2O_4$; Hollow microspheres; High power; Long life

1. INTRODUCTION

Lithium-ion batteries are considered as one of the most promising energy storage devices and have gained enormous interest recently for large-scale application, such as electric vehicles (EV) and hybrid electric vehicles (HEV). At present, the mainly cathode material is $LiCoO_2$, which has high theoretical capacity and good cycling stability, but possess high cost and toxicity of Co [1]. For this reason, spinel $LiMn_2O_4$ has been studied as the most promising cathode material for lithium ion batteries, which has low cost, acceptable environmental impact, high electric potential and high safety [2-3]. Unfortunately, $LiMn_2O_4$ shows severe capacity fading during cycling, which is mainly due to the

dissolution of Mn into the electrolytes at elevated temperature and Jahn-Teller effect [4]. The poor power density and large polarization effect have largely hindered its application in high power lithium ion batteries, which are due to slow diffusion and long diffusion distance in active material. Hence, it is still necessary to improve its cycling stability and high rate capability.

Nanostructured spinel $LiMn_2O_4$ with various morphologies have been extensively prepared to improve its cycle performance and rate capability for lithium ion batteries, such as nanoparticles [5], nanowires [6] and nanorods [7]. But these nanostructured $LiMn_2O_4$ with high specific surface leads to higher surface reactivity, which causes dissolution of Mn into the electrolytes quickly. It is found that the electrochemical performance of $LiMn_2O_4$ electrodes appreciably depends on the morphology, the particle size and the porosity of the structure. $LiMn_2O_4$ hollow microspheres exhibit better rate capability and cycle stability [8]. Hollow structure can buffer structural stress in long-term charge-discharge process and provide more osmotic space between active materials and electrolyte, which brings about high rate capability and excellent cycle performance. Bruce et al. [9] have reported that ordered mesoporous $Li_{1.12}Mn_{1.88}O_4$ show the high rate capability (70 $mAhg^{-1}$ at 3000 mAg^{-1}).

For hollow structure $LiMn_2O_4$, the synthesis method used is mainly template method [10-13]. Generally speaking, hard templates are difficult to remove clean. So self-template method is more suitable for preparation of hollow structure $LiMn_2O_4$. Self-template not only acts as reactant precursor, but also acts as template in reaction. What's more, it is easy to obtain stable hollow structure with any further treatment. In this work, the spinel $LiMn_2O_4$ hollow microspheres were synthesized by using $MnCO_3$ microsphere as a self-sacrificial template. The electrochemical performance of $LiMn_2O_4$ hollow microspheres was investigated in detail.

2. EXPERIMENTAL PART

2.1 Synthesis of $LiMn_2O_4$ hollow microspheres

$MnCO_3$ microspheres were synthesized by a precipitation method reported [14] with modifications. In a typical experiment, $MnSO_4 \cdot H_2O$, NH_4HCO_3 and $(NH_4)_2SO_4$ were separately dissolved in distilled water. Ethanol (7 mL), NH_4HCO_3 solution, and $(NH_4)_2SO_4$ solution were then added to the $MnSO_4 \cdot H_2O$ solution in sequence under stirring. The total concentration of $MnSO_4 \cdot H_2O$, NH_4HCO_3 and $(NH_4)_2SO_4$ is 0.1 M and 1.0 M, respectively. The prepared $LiMn_2O_4$ hollow microspheres are entitled LMO-0.1M and LMO-1.0M. The precipitation was performed by maintaining the mixed solution at 50 ^oC for 7 hours. Then $MnCO_3$ microspheres were obtained by filtering, washing and drying in a vacuum at 60 ^oC overnight.

The obtained $MnCO_3$ microspheres are used as self-templates for preparing $LiMn_2O_4$ hollow microspheres. Firstly, the MnO_2 microspheres were synthesized by thermal decomposition of the $MnCO_3$ microspheres at 350 ^oC for 8 hours. Then MnO_2 microspheres were mixed with $LiOH \cdot H_2O$ with the molar ratio of 2:1.05 in ethanol. The ethanol was evaporated slowly at room temperature under stirring. The mixture of obtained was ground manually for 10 minutes and then calcined at 750

^{o}C for 10 hours in air to obtain $LiMn_2O_4$ hollow microspheres. For comparison, $LiMn_2O_4$ particles were also prepared by sintering the mixture of MnO_2 and $LiOH \cdot H_2O$ at 800 ^{o}C for 10 hours in air.

2.2 Characterization of $LiMn_2O_4$ hollow microspheres

The crystal structure of the products was characterized by X-ray diffraction (XRD) with Cu Kα radiation at a voltage of 40 kV and a current of 40 mA. The morphologies of the products were examined by a field-emission scanning electron microscope (Hitachi S4800).

2.3 Electrochemical properties measurements

The electrochemical tests were carried out by using CR2032 coin-type cells with lithium metal as the negative electrode. The cathode was prepared by mixing the active material, acetylene black (AB) and polyvinylidene fluoride (PVDF) with a weight ratio of 8:1:1. The cell assembly was operated in a glovebox filled with pure argon. The electrolyte was 1M $LiPF_6$ dissolved in ethylene carbonate (EC)/dimethyl carbonate (DMC) (1:1 in volume). Galvanostatic charge/discharge measurements were performed between 3.0 and 4.4 V at different current densities (1C rate corresponds to the current density of 148 mAg^{-1}). Cyclic voltammetry (CV) analyses were recorded on a Solartron Modulab 2100A electrochemical station. The electrochemical behaviors of Li^+ ions insertion/extraction into/from the spinel $LiMn_2O_4$ take place within the potential range between 3.9 and 4.2 V versus Li/Li^+ [15], In addition, a Jahn-Teller distortion is introduced into the spine1 structure reducing the crystal symmetry from cubic to tetragonal when $LiMn_2O_4$ is deeply discharged to 3 V, resulting in the capacity decay and poor cycling stability [16]. So the sweep potential range of CV is chosen between 3.4 and 4.3 V in this work.

3. RESULTS AND DISCUSSION

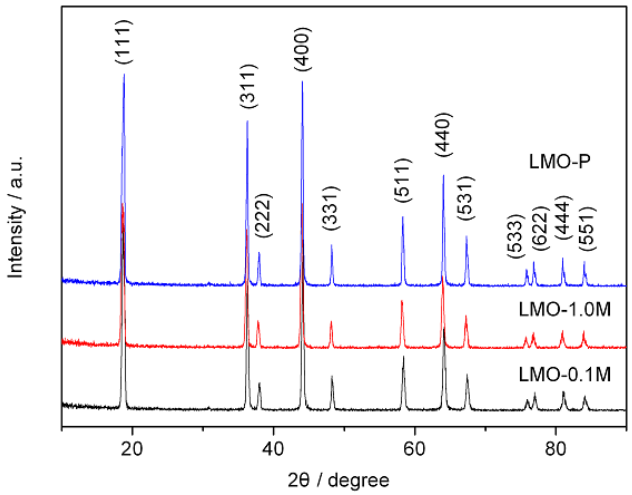

Figure 1. XRD patterns of $LiMn_2O_4$ microspheres.

Fig.1 shows the XRD patterns of the $LiMn_2O_4$ powders. All the diffraction peaks can be indexed as spinel $LiMn_2O_4$ (JCPDS No. 35-0782), without the appearance of any unknown diffraction peak. The results demonstrate the high purity and well crystallinity of the as-synthesized spinel $LiMn_2O_4$.

The morphology and particle size of the products are examined by field-emission scanning electron microscope (FE-SEM), as shown in Fig. 2. The FE-SEM images reveal that the product is composed of uniform hollow microspheres with diameters of 0.5 – 2.0 μm. From the broken microspheres, the hollow microspheres are composed of nanobuilding blocks with a size of 50 – 300 nm. The size of nanobuilding blocks in LMO-0.1M products is smaller than that of LMO-1.0M products.

The formation of $LiMn_2O_4$ hollow microspheres is mainly attributed to porous microsphere MnO_2 [14]. According to the thermogravimetric analysis (TGA) curve of the $MnCO_3$, the $MnCO_3$ microspheres are converted into MnO_2 porous microsphere by thermal decomposition at 350 ^oC because of the release of CO_2. During the sintering process, the microsphere morphology is retained. The fusion of the mesopores and a mechanism analogous to the Kirkendall effect may lead to the formation of the hollow architecture of $LiMn_2O_4$ microspheres [17].

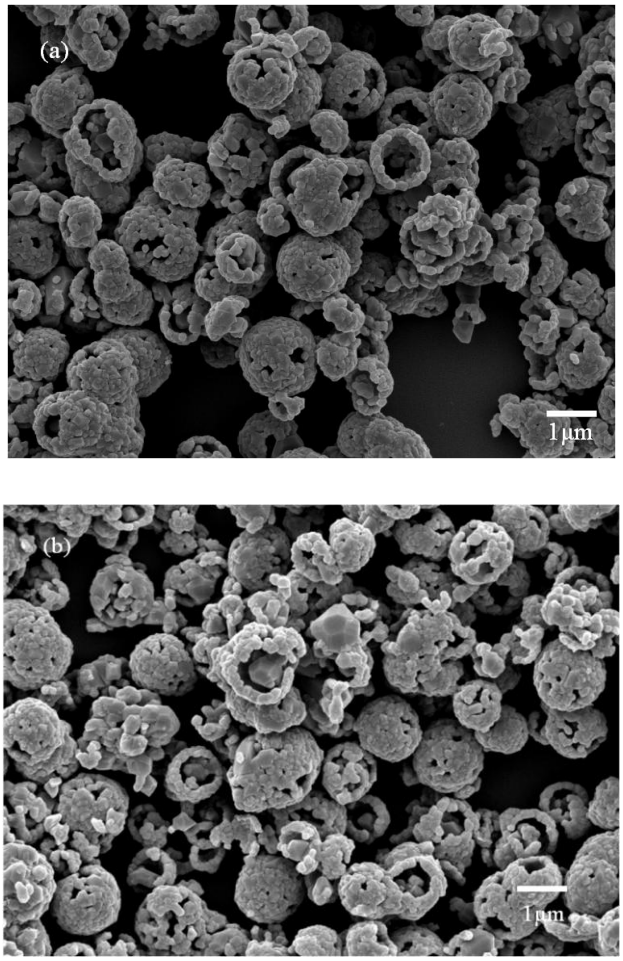

Figure 2. FE-SEM images of (a) LMO-0.1M and (b) LMO-1.0M hollow microspheres.

The 100th charge-discharge curves of LMO-P, LMO-0.1M, and LMO-1.0M at a rate of 10C are shown in Fig.3(a). The discharge specific capacities of LMO-P, LMO-0.1M, and LMO-1.0M are 48.1, 70.8 and 76.2 mAhg^{-1}, respectively. It is obvious that the LMO-1.0M has much better high-rate capability than that of LMO-P and LMO-0.1M. The superior high-rate capability for LMO-1.0M hollow microspheres may be due to their hollow structure being extraordinarily suitable for lithium ion diffusion. On the other hand, LMO-0.1M hollow microspheres consisted of the smaller nanopaticles with high specific surface leads to higher surface reactivity, which causes larger dissolution of Mn into the electrolytes, then the inferior high-rate capability.

All three samples show excellent cycling stability at the charge-discharge rate of 10C, as shown in Fig.3(b). The initial discharge capacities are 49.7, 74.3 and 84.4 mAhg^{-1} for LMO-P, LMO-0.1M and LMO-1.0M, respectively. After 1000 cycles, the corresponding discharge capacities are 43.9, 62.2 and 67.8 mAhg^{-1}. Especially, the capacity retention ratio of the LMO-1.0M sample is 75.4% after 2000 cycles (see Fig.3(c)). The results indicate that the hollow microspheres show excellent high-rate capability and cycling stability. Moreover, the preparation of $LiMn_2O_4$ hollow microspheres under solution concentration of 1.0M can realize their commercial production.

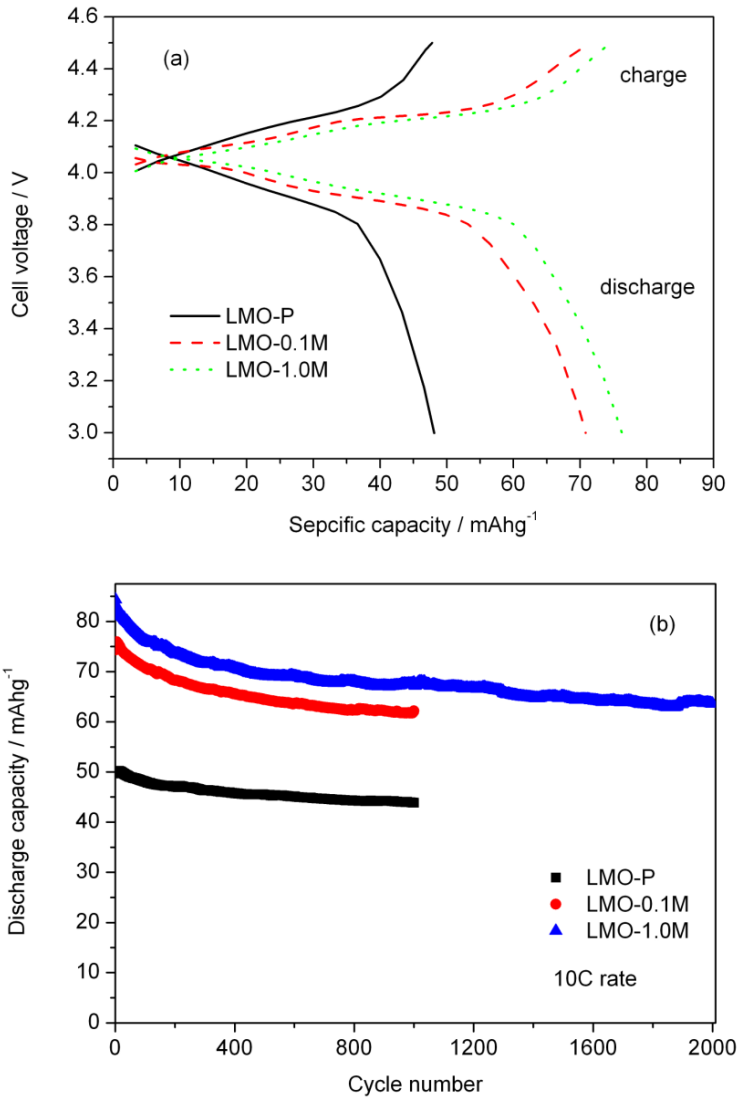

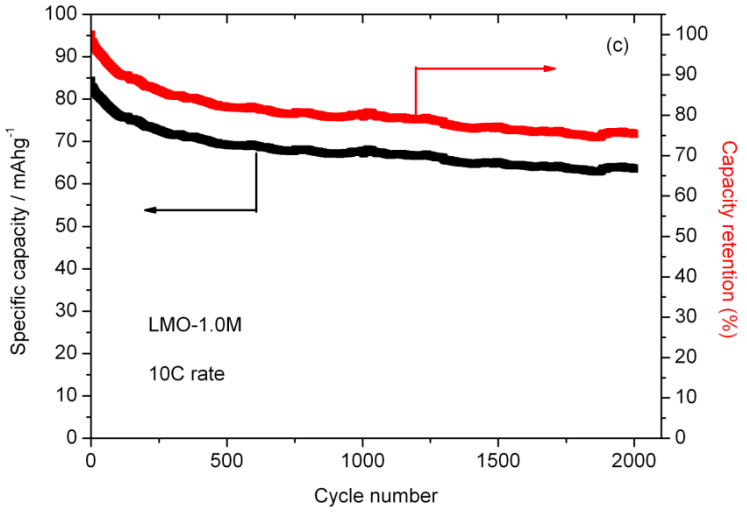

Figure 3. (a) The 100th charge/discharge curves of LMO-P, LMO-0.1M and LMO-1.0M at 10C rate between 3.0 V and 4.5 V, (b) the cycling stability of three samples, (c) the capacity retention of LMO-1.0M hollow microspheres.

Fig.4 (a) shows the cyclic voltammograms of the LMO-1.0M sample at different scan rates. The peak current increases with the increase of scan rates. Two pairs of separated redox peaks can be clearly observed, suggesting that lithium ions are extracted or inserted from/into $LiMn_2O_4$ with a two-step mechanism [13, 18]. It is noted that the LMO-1.0M sample exhibits higher symmetrical redox peaks than LMO-P sample, revealing favourable extraction/insertion reversibility of lithium ion in the $LiMn_2O_4$ hollow microspheres.

Figure 5(a) presents the discharge curves for LMO-1.0M hollow microspheres under different charge-discharge current rates. At low rate, it clearly display two plateaus at about 4.1 and 4.0 V vs. Li/Li^+, indicating a two-step process during cycling, which corresponds to the two pairs of redox peaks in the CV plots. As the current rate increasing, the plateau voltages shift toward lower potential, and separation of the two discharge plateaus become undistinguished due to increased cell polarization at high current rates. In figure 5(b), discharge capacity retention as a function of cycle number for LMO-1.0M microspheres at 20C rate is shown. After 1200 cycles, it still maintains excellent cycle stability. The initial capacity is 61.5 $mAhg^{-1}$, and the final capacity is 53.9 $mAhg^{-1}$. The capacity retention is about 87.6% after 1200 cycles. The excellent electrochemical performance for the LMO-1.0M microspheres can be attributed to its hollow structure. The hollow structure can enhance the contact between active materials and the electrolyte, and is beneficial to penetration of the electrolyte into the whole microspheres, which can contribute to excellent rate capability and high gravimetric capacity [12]. On the other hand, it can buffer against volume changes during Li^+ ions insertion/extraction processes leading to the long-term cycling stability.

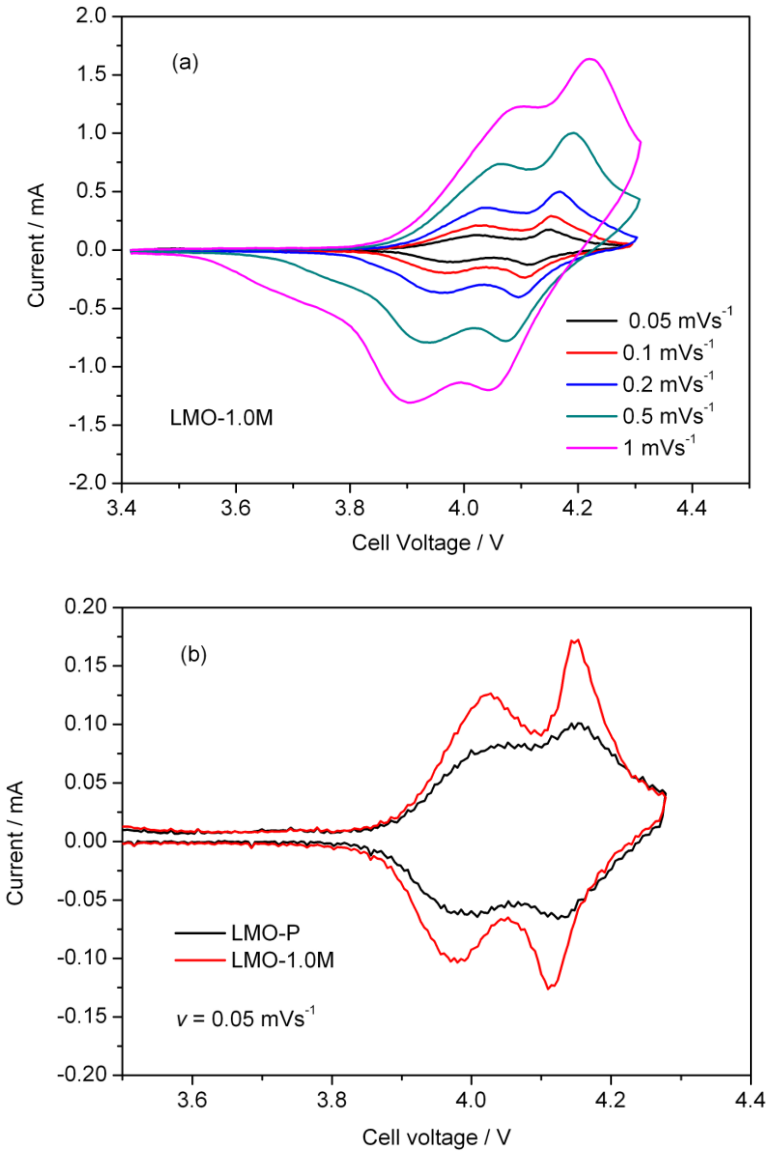

Figure 4. (a) Cyclic voltammograms of the LMO-1.0M sample at different scan rates, (b) Cyclic voltammograms of the LMO-P and LMO-1.0M samples at a scan rate of 0.05 mVs^{-1}.

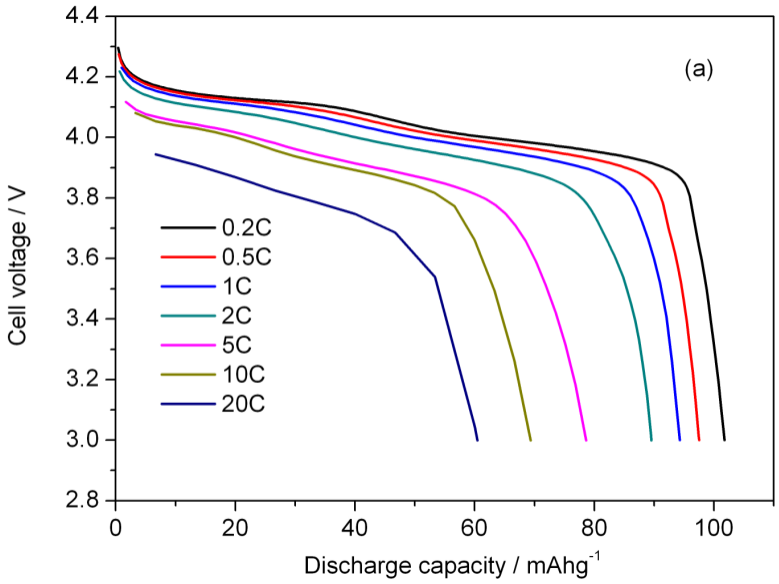

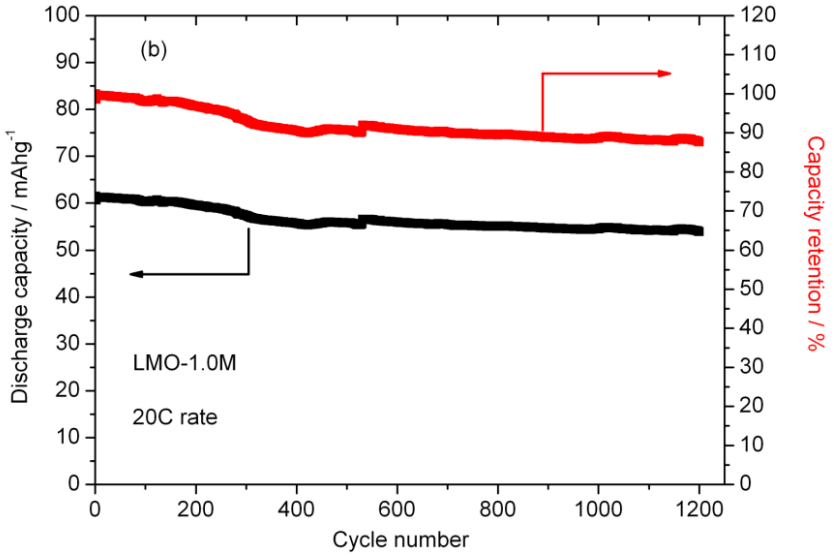

Figure 5. (a) The discharge curves for LMO-1.0M hollow microspheres under different current rates, (b) discharge capacity retention as a function of cycle number for LMO-1.0M microspheres at 20C rate.

4. CONCLUSIONS

$LiMn_2O_4$ hollow microspheres were successfully prepared using $MnCO_3$ microspheres as self-sacrificial template. The results show that the $LiMn_2O_4$ hollow microspheres possess excellent rate capability and high cycling stability. The electrochemical performance is better than that of $LiMn_2O_4$ particles. For the LMO-1.0M sample the discharge capacity is 53.9 $mAhg^{-1}$ after 1200 charge-discharge cycles at a rate of 20C and the capacity retention is about 87.6%, indicating the $LiMn_2O_4$ hollow microspheres have a great application prospect in high-power lithium ion batteries.

ACKNOWLEDGMENT
This research is jointly supported by the program of Guangxi Natural Science Foundation (Project No. 2012GXNSFBA053154 and 2012GXNSFGA060002) and the Research Foundation of Education Bureau of Guangxi Zhuang Autonomous Region, China (Project No. 201101ZD007).

References

1. Y.K. Sun, C.S. Yoon, C.K. Kim, S.G. Youn, Y.S. Lee, M.Yoshio and I.H. Oh, *J. Mater. Chem.*,11 (2001) 2519.
2. J.M. Tarascon, E. Wang, F.K. Shokoohi, W.R. Mckinnon and S. Colson, *J. Electrochem. Soc.*, 138 (1991) 2859.
3. J.M. Tarascon and D. Gguyomard, *Electrochim. Acta.*, 38 (1993) 1221.
4. C.H. Lu and S.W. Lin, *J. Power Sources*, 97-98 (2001) 458.
5. M.S. Whittingham, *Chem. Rev.*, 104 (2004) 4271.
6. Y. Wang and G.Z. Cao, *Adv. Mater.*, 20 (2008) 2251.
7. Y.G. Guo, Y.S. Hu and W. Sigle and J. Maier, *Adv. Mater.*, 19 (2007) 2087.

8. A.S.Aricò, P. Bruce, B. Scrosati, J.M. Tarascon and W. Van Schalkwijk, *Nat. Mater.*, 4 (2005) 366.
9. P.G. Bruce, B. Scrosati and J.M. Tarascon, *Angew. Chem.*, 120 (2008) 2972.
10. K.M. Shaju and P.G. Bruce, *Chem. Mater.*, 20 (2008) 5557.
11. X. Xiao, J. Lu and Y. Li, *Nano Res.*, 3 (2010) 733.
12. Y.L. Ding, X.B. Zhao, J. Xie, G.S. Cao, T.J. Zhu, H.M. Yu and C.Y. Sun, *J. Mater. Chem.*, 21 (2011) 9475.
13. C.Y. Sun, H.Y. Yang, J. Xie, G.S. Cao, X.B. Zhao and T.J. Zhu, *Int. J. Electrochem. Sci.*, 7 (2012) 6191.
14. L. Zhou, D. Zhao, and X.W. Lou, *Angew. Chem. Int. Ed.*, 50 (2011) 1.
15. C.H. Jiang, S.X. Dou, H.K. Liu, M. Ichihara and H.S. Zhou, *J. Power Sources*, 172 (2007) 410.
16. R.J. Gummow, A. de Kock and M.M. Thackeray, *Solid State Ionics*, 69 (1994) 59.
17. X.W. Lou, L.A. Archer and Z.C. Yang, *Adv. Mater.*, 20 (2008) 3987.
18. Y. Xia and M. Yoshio, *J. Electrochem. Soc.*, 143 (1996) 825.